

Density functional theory study of a graphene sheet modified with titanium in contact with different adsorbates

M. I. Rojas and E. P. M. Leiva*

INFIQC, Unidad de Matemática y Física, Facultad de Ciencias Químicas, Universidad Nacional de Córdoba, Ciudad Universitaria, 5000 Córdoba, Argentina

(Received 16 February 2007; revised manuscript received 31 May 2007; published 17 October 2007)

The present work is based on the theoretical study of the behavior of a graphene sheet decorated with titanium, in contact with different molecules. When the substrate is exposed only to hydrogen molecules, it is found to store up to four molecules per adatom, as already seen in the literature for single wall carbon nanotubes. Thus, titanium decoration is seen to considerably improve the hydrogen storage capacity of these carbon systems. However, it is found that low quantities of oxygen present in the gas phase should yield the oxidation of the titanium atoms, even when hydrogen is stored in the system. It is concluded that if the experimental system is exposed to air, titanium atoms on these surfaces are expected to oxidize to titanium dioxide, showing oxygen molecules to be very reactive species. Other chemicals present in air such as nitrogen or water molecules could also be chemisorbed onto the titanium adatom, but are less competitive with hydrogen.

DOI: [10.1103/PhysRevB.76.155415](https://doi.org/10.1103/PhysRevB.76.155415)

PACS number(s): 73.22.-f, 68.43.Bc, 68.43.Fg, 73.20.Hb

INTRODUCTION

Single wall carbon nanotubes (SWCNTs) are graphene sheets rolled up into a compact tube of finite diameter. The lengths may vary from a few nanometers up to hundreds of microns or even centimeters.¹ Depending on the direction of the folding, they have different electronic properties (insulating, semimetallic, or metallic) and are named as (m,n) .² These indices determine the diameter of the nanotube and their chirality.

The progress in the synthesis of these novel carbon compounds by laser ablation method and chemical vapor deposition have facilitated the study of their properties and applications.³⁻⁵ Nanotubes can be decorated with different transition metals by electron-beam deposition in ultrahigh vacuum conditions. In the case of the titanium deposit, a continuous Ti nanowire deposited on SWCNT⁶ has been reported.

Among other properties, SWCNTs are of technological importance since they may be suitable for gas storage. This property is especially worth analyzing in the case of hydrogen storage, since this gas is the optimal candidate as energy carrier in an economy based on renewable resources.

Recent computational studies have shown that titanium decoration of SWCNTs remarkably increases the hydrogen storage capacity from the gas phase, allowing its storage of up to four hydrogen molecules per Ti adatom.^{7,8} Thus, the titanium decoration would considerably improve the hydrogen storage capacity of the carbon systems.

However, the obvious question arising from practical applications is the probability that the deposit is titanium or titanium dioxide, taking into account the experimental conditions. From general chemistry, it is known that the oxygen molecule is a very reactive species, present in air with a concentration of approximately 20%. Nanotube modifications are performed in ultrahigh vacuum conditions. However, even when the system is evacuated, it never becomes completely free of oxygen, leaving an air pressure of

$\sim 10^{-15}$ atm. For this reason, the study of the interaction of the system with the oxygen molecule is of potential technological relevance, since the small amount of oxygen present in the gas phase could give way to titanium oxidation. If this process occurs before hydrogen storage, then the oxidized titanium on the surface of the nanotube could have very different properties from those expected for the Ti. On the other hand, even if hydrogen could be stored on an oxygen-free system, the Ti decoration exposed to a small amount of oxygen will be inevitably oxidized, with the consequent reduction of the storage capacity. For this reason, the oxidation of the Ti decoration needs to be considered. Other molecules in the air such as nitrogen or water could be chemisorbed onto the titanium adatom, these competitive processes also being of potential interest.

In this work, we attempt to contribute to the understanding of the behavior of Ti modified carbon nanotubes exposed to the air components by means of density functional theory (DFT) calculations. As the Ti/nanotubes require a large number of atoms to be represented, we decided to work with a titanium modified graphene sheet, because this system has lower computational requirements. To test this approach, calculations for hydrogen adsorption on Ti/graphene were performed in comparison with previous results for adsorption on Ti/SWCNT.⁶ Our results show that calculations with the graphene layer should deliver a good estimation of the reactions that can occur on the modified nanotubes. In addition, the oxidation of the Ti decoration in the presence of physically adsorbed hydrogen has been considered. This should represent a situation where a Ti-containing nanotube with hydrogen stored on it is exposed to small amounts of oxygen. The effect of other substances in air, like nitrogen or water that could be chemisorbed on titanium, has also been analyzed.

MODEL AND COMPUTATIONS

The graphene sheet was represented by a basis of 24 carbon atoms, distributed in a honeycomb arrangement. The ti-

TABLE I. Parameters employed in the present calculations. r_{nl} represents the cutoff radius of the pseudo-potentials. In the basis, the single and double zeta orbitals of a given angular momentum have the following parameters: r_i , $r_{c,1}$, and $r_{c,2}$, which are the inner radius and the cutoff radii of the first and second zeta for a given angular momentum, respectively. All radii are expressed in bohr. δQ and V_0 represent the extra charge (a.u.) and the prefactor of the soft confinement potential (Ry), respectively.

Symbol	Pseudopotential radius	Basis	
		δQ	Soft confinement parameters
H	r_{1s} 0.63 r_{2p} 1.15 r_{3d} 1.29 r_{4f} 1.82	0.002	$1s$ $\begin{cases} V_0 & 11.10 \\ r_i & 0.44 \\ r_{c,1} & 9.00 \\ r_{c,2} & 2.60 \end{cases}$
O	r_{2s} 0.65 r_{2p} 0.65 r_{3d} 0.95 r_{4f} 2.00	0.017	$2s$ $\begin{cases} V_0 & 0.63 \\ r_i & 2.50 \\ r_{c,1} & 6.30 \\ r_{c,2} & 2.97 \end{cases}$ $2p$ $\begin{cases} V_0 & 0.73 \\ r_i & 4.73 \\ r_{c,1} & 6.00 \\ r_{c,2} & 2.70 \end{cases}$
N	r_{2s} 0.85 r_{2p} 1.17 r_{3d} 1.18 r_{4f} 2.00	0.028	$2s$ $\begin{cases} V_0 & 0.60 \\ r_i & 2.45 \\ r_{c,1} & 6.28 \\ r_{c,2} & 2.82 \end{cases}$ $2p$ $\begin{cases} V_0 & 0.57 \\ r_i & 4.25 \\ r_{c,1} & 5.47 \\ r_{c,2} & 2.65 \end{cases}$
C	r_{2s} 1.25 r_{2p} 1.25 r_{3d} 1.25 r_{4f} 1.25	0.428	$2s$ $\begin{cases} V_0 & 148.37 \\ r_i & 9.33 \\ r_{c,1} & 8.99 \\ r_{c,2} & 5.07 \end{cases}$ $2p$ $\begin{cases} V_0 & 2.20 \\ r_i & 5.22 \\ r_{c,1} & 7.30 \\ r_{c,2} & 2.87 \end{cases}$ $3d$ $\begin{cases} V_0 & 25.97 \\ r_i & -0.12 \\ r_{c,1} & 3.34 \end{cases}$
Ti	r_{4s} 1.93 r_{4p} 2.25 r_{3d} 1.31 r_{4f} 1.98	0.011	$4s$ $\begin{cases} V_0 & 50.77 \\ r_i & 28.48 \\ r_{c,1} & 9.29 \\ r_{c,2} & 7.02 \end{cases}$ $4p$ $\begin{cases} V_0 & 53.48 \\ r_i & 10.59 \\ r_{c,1} & 13.09 \\ r_{c,2} & 2.81 \end{cases}$ $3d$ $\begin{cases} V_0 & 16.36 \\ r_i & 4.89 \\ r_{c,1} & 5.83 \\ r_{c,2} & 3.62 \end{cases}$

tanium decoration was represented by one titanium atom adsorbed on a hollow site. The unit cell was tetragonal $7.39 \times 8.53 \times 20 \text{ \AA}^3$ with periodic boundary conditions in x, y, z in order to represent an infinite sheet. As we model the solid/vacuum interphase, we choose a big modulus unit cell vector in the z direction, so that the interactions between the system and their images become negligible.

We performed calculations with unit cells of smaller and larger sizes. Within this set, we chose the 24 atom one because it was found to be more adequate for the present purposes. The optimal supercell must have low Ti-Ti interactions and a reasonable number of atoms to demand an affordable computational cost. Test runs with a 96 atom unit cell showed changes lower than 0.10 eV for the binding energies of the small molecules and even lower changes for the activation barriers.

For these systems, DFT calculations were performed employing the SIESTA computer code.^{9,10} A localized basis set composed of double- ζ plus polarization was used. The basis functions were numerical atomic orbitals (NAOs), the solutions of the Kohn-Sham Hamiltonian for the isolated pseudoatoms. Exchange and correlation effects were described using a generalized gradient approximation, within the Perdew-Burke-Ernzerhof functional.¹¹ The core electrons

were replaced by norm conserving pseudopotentials¹² in their fully separable form.¹³ The nonlinear exchange-correlation correction¹⁴ was included for Ti to improve the description of the core valence interactions. In the pseudo-potential description of the atoms, the following valence electronic states were considered: Ti, $4s^2 3d^2 4p^0$; C, $2s^2 2p^2 3d^0$; H, $1s^1$; and O, $2s^2 2p^4$. In order to obtain orbitals with continuous derivatives, a soft confinement potential was employed.¹⁵ The value of the confinement parameters were defined variationally employing the simplex method.¹⁶ All the parameters used in the calculations are listed in Table I.

As the SIESTA employed NAOs, the program replaces some integrals in real space by sums in a finite three dimensional real space grid, controlled by one single parameter, the energy cutoff of the grid.⁹ This cutoff, which refers to the fineness of the grid, was converged for all the systems studied here, finding suitable a value of 150 Ry.

The study of the minimum energy path for the different reactions was undertaken using the nudged elastic band (NEB) method,^{17,18} and the local minima were found through the conjugate gradient (CG) technique, employing DFT calculations with spin polarization (SP).

RESULTS AND DISCUSSIONS

A graphene sheet was employed to emulate a nanotube because it is a smaller system and allowed making NEB and CG-DFT SP calculations with minimal computational effort. As starting point, the graphene sheet was studied by means of CG minimization. The lattice parameter obtained by energy minimization was equal to 2.459 Å (the experimental value for graphite crystal¹⁹ is 2.456 Å) with zero total spin polarization.

The graphene sheet was then decorated with Ti. The adatom adsorbed on a hollow site yielded an average bond distance $d_{C-Ti}=2.34\pm 0.01$ Å with a binding energy of $E_B=-1.51$ eV. Yildirim and Ciraci⁸ obtained a binding energy value of -2.2 eV for Ti adsorption on an (8,0) SWCN, this value being reduced to -1.8 eV for a (12,0) SWCN and to -1.6 eV for a (7,7) SWCN, so that we can consider that the present calculations are in good agreement with the previous ones. The system presented a total spin polarization equal to $3.30\mu_B$ (Bohr magnetons). From Mulliken population analysis, it was found that the Ti atom presents a net charge equal to $+0.456$, while the neighboring C atoms present negative ones with values between -0.005 and -0.050 .

Hydrogen adsorption

Figure 1(a) shows the energy of the system for adsorption of a hydrogen molecule on the Ti-graphene layer along the CG minimization steps. During the minimization, the hydrogen molecule approaches the surface from the vacuum side, on a location that is adjacent to the titanium atom, obtaining a fast energy decrease. At -0.20 eV, the H_2 molecule starts to tilt and the energy decreases with a smaller slope. At -0.22 eV, there is a break point in the energy minimization curve, when the molecule begins to rotate next to the titanium atom, searching a better overlap until the end of the minimization yielded hydrogen molecular adsorption with a binding energy of -0.42 eV. The adsorbed hydrogen molecule has a larger H-H distance $d_{H-H}=0.87$ Å than the non-interacting one, which is $d_{H-H}=0.76$ Å as calculated by the present methodology (the experimental distance measured in the gas phase is equal to $d_{H-H}=0.74$ Å, Ref. 20).

In order to study the dissociation of a single hydrogen molecule onto the Ti/graphene system, we determined the equilibrium configuration of the dissociated state by CG minimization. In the equilibrium configuration, the two H atoms adsorbed on the Ti are separated by a distance of $d_{H-H}=3.09$ Å, the average distance between the H and Ti atoms is $d_{H-Ti}=1.78\pm 0.01$ Å, and the hydrogen and Ti atoms form an angle $\text{Ti}-\angle_{H}^H$ of 120.8° .

Since in the first CG minimization the dissociation did not occur, we inferred that the dissociation reaction involves an energy barrier. For this reason, we employed the NEB method to determine the reaction path. Figure 1(b) shows the energy as a function of the reaction coordinate. The energy difference between the adsorbed molecular state (initial state) and the adsorbed atomic state (final or dissociated state) was found to be -0.50 eV in favor of the latter, with an energy barrier of 1.24 eV. When the adsorption energy of hydrogen in the molecular state is added to the energy of the

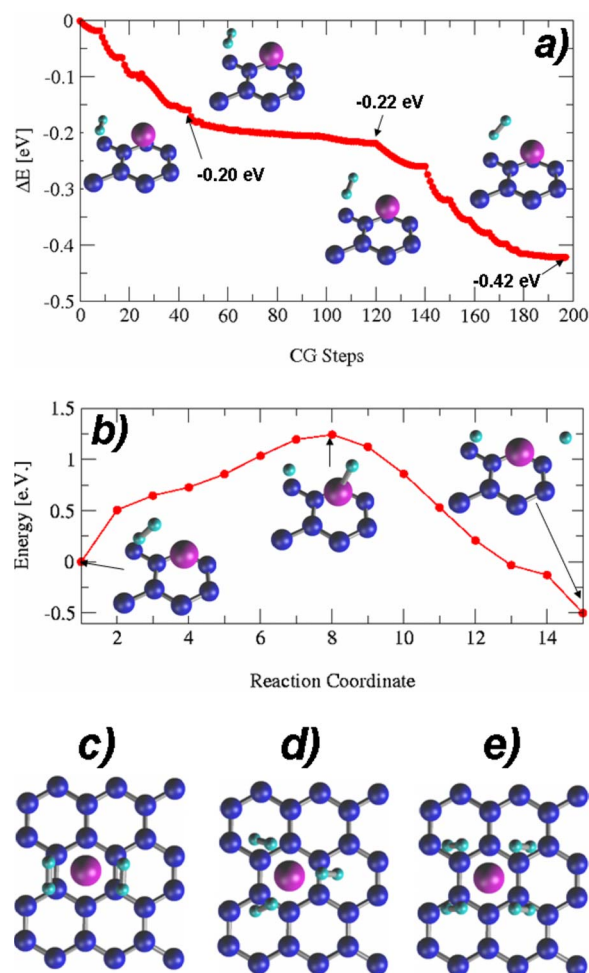


FIG. 1. (Color online) Hydrogen adsorption onto Ti/graphene. (a) CG energy changes in (eV) as a function of the minimization steps. The energy zero is taken to be the hydrogen molecule infinitely far from the rest of the system. (b) Energy along reaction coordinate obtained with the NEB method for the hydrogen molecule dissociation process. The energy zero corresponds to the initial state as depicted in the figure. CG equilibrium configurations for multiple hydrogen molecules adsorbed onto Ti/graphene system, in the case of (c) two, (d) three, and (e) four H_2 molecules: Blue, C; magenta, Ti; and cyan, H.

dissociation process, the resulting total energy of adsorption is -0.92 eV.

The maximum number of H_2 molecules that a Ti adatom can coordinate was analyzed by means of CG calculations. It was found that each Ti can adsorb up to four molecules. Attempts to obtain a larger coordination number yielded desorption of the excess molecules. Figures 1(c)–1(e) show top views of the equilibrium configurations for the adsorption of two, three, and four H_2 molecules, respectively.

Although they suggest that the hydrogen arrangements are related to the structure of the sheet, it must be kept in mind that the interaction is mainly with the titanium atom and not with the sheet. The resulting adsorption energies per molecule are -0.42 or -0.92 eV for one molecular or dissociated adsorption and -0.46 , -0.56 , and -0.42 eV/ H_2 molecule in the case of two, three, and four molecules, respectively.

These values can be compared with those for the nanotube case given in Ref. 8. These authors found an adsorption energy of -0.83 eV for a single H_2 molecule in a dissociated state and a value of -0.54 eV/ H_2 molecule for four H_2 molecules adsorbed in a symmetric configuration, very similar to that shown in Fig. 1(e). These magnitudes of the binding energies suggest that the hydrogen molecules are physisorbed rather than chemisorbed on the Ti/graphene layer. These conditions appeared optimal for a storage system, since the hydrogen molecules could be recovered in the gas state by warming up the system, as found by Yildirim and Ciraci *et al.*⁸ in a molecular dynamics simulation at 800 K.

Ti oxidation reaction

It is known from theoretical calculations in previous work²¹ that in vacuum the ground state geometry of the TiO_2 molecule presents a bent structure with a Ti-O bond distance of 1.65 Å and a bond angle $\angle O-Ti-O$ of 114.2° .

In our study of the interaction between an oxygen molecule and the Ti/graphene system, some attack directions must be taken into account to emulate the entrance of the oxygen molecule into the system. Depending on the attack direction, we found that the titanium dioxide remains adsorbed on the graphene sheet on different sites and with different positions.

Figure 2(a) shows a CG minimization for an oxygen molecule that comes from the vacuum side perpendicular to the graphene surface on top of the Ti atom. In the minimization curve, the energy decreases steeply as the oxygen molecule approaches the Ti atom. The distance between the two oxygen atoms increases from 1.28 Å (noninteracting) to $d_{O-O} = 1.54$ Å (adsorbed molecule), and the average Ti-O distance is $d_{Ti-O} = 1.89 \pm 0.01$ Å. The end point of the minimization corresponds to a molecular adsorption with a binding energy of -4.66 eV. The initial and final geometries are included along with the CG minimization curve in Fig. 2(a).

As was expected that Ti formed TiO_2 with O_2 , we also considered an adsorbed dissociated state for O_2 by CG minimization. The energy gain to reach this state is -7.75 eV with respect to an O_2 molecule considered not interacting with the Ti/graphene sheet. The $O-O$ and the average Ti-O distances were $d_{O-O} = 2.85$ Å and $d_{Ti-O} = 1.69 \pm 0.01$ Å, respectively.

Figure 2(b) shows the reaction path between molecular adsorption (initial state) and dissociation (final state) with an energy difference of -3.09 eV. The reaction path between these two states was obtained using the NEB method. The barrier is 0.06 eV high, a very low value. Thus, this is practically a nonactivated process and it is expected to occur spontaneously at room temperature. The reconstruction of the oxygen molecule (reverse reaction) has an energy barrier of 3.15 eV.

If we compare the energy gain for the oxygen molecular adsorption of -4.66 eV with that for adsorption in the dissociated state of -7.75 eV, we conclude that if the Ti/graphene sheet is brought into contact with a small amount of oxygen, it is expected that the Ti adatom should oxidize to TiO_2 in a spontaneous irreversible process. A separate calculation of the energy change for the reaction

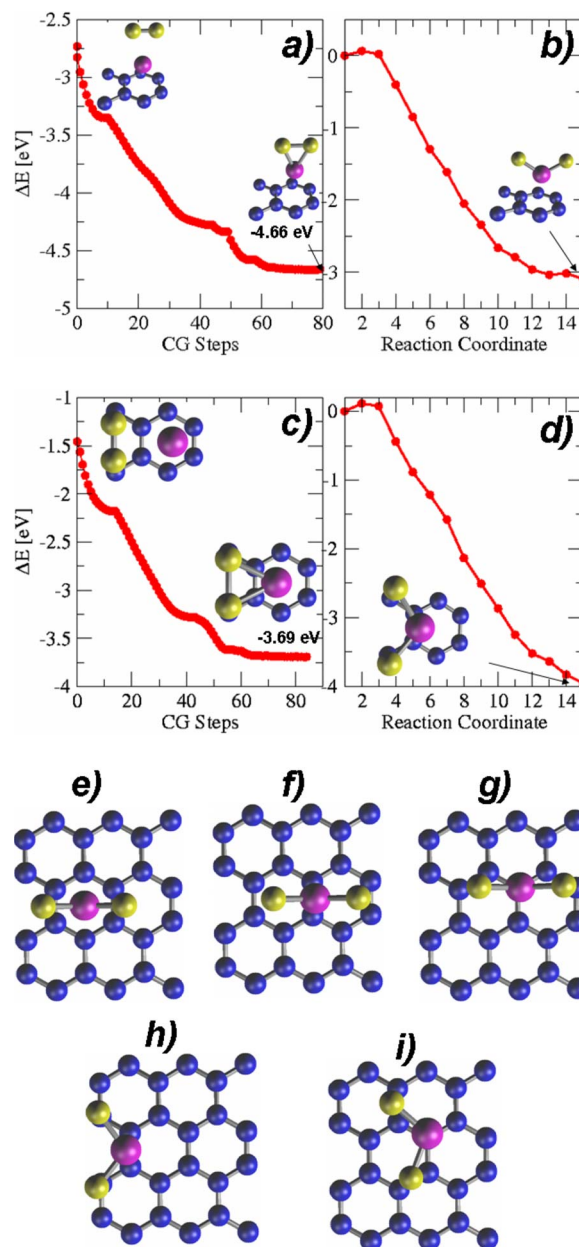
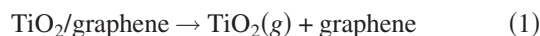


FIG. 2. (Color online) [(a) and (c)] Energy as a function of CG steps for O_2 molecular adsorption on the titanium adatom/graphene system through different approach directions. (a) corresponds to a direction perpendicular to the surface, (c) to a direction parallel to the graphene sheet. [(b) and (d)] Energy along the reaction path for dissociation of the O_2 molecule on the titanium adatom/graphene system to yield TiO_2 , as obtained using the nudged elastic band method. (b) corresponds to a direction perpendicular to the surface, (d) to a direction parallel to the graphene sheet. Different geometries of the TiO_2 species considered for the calculations of the O_2 and TiO_2 binding energies reported in Table II: (e) hollow, (f) bridge, (g) top, (h) rotated bridge, and (i) rotated top. Blue, C; magenta, Ti; and yellow, O.



shows that the TiO_2 entity remains adsorbed on graphene in the hollow site with a binding energy of -1.55 eV.

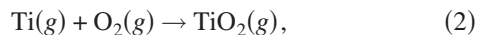
TABLE II. Binding energy E_{O_2} of a dissociated oxygen molecule adsorbed on Ti/graphene, with the geometries described in Figs. 2(e)–2(i). E_{TiO_2} denotes the binding energy of the TiO_2 species to the surface.

Adsorption type	E_{O_2} (eV)	E_{TiO_2} (eV)
Hollow	-7.75	-1.55
Bridge	-7.78	-1.58
Top	-7.69	-1.49
Rotated bridge	-7.64	-1.44
Rotated top	-7.82	-1.62

The previous results for O_2 adsorption were obtained when the O_2 molecule was introduced perpendicularly to the surface, right on top of the Ti atom. Figure 2(c) shows the CG energy minimization curve when the O_2 molecule comes close to the Ti atom from an adjacent side in a parallel direction to the graphene sheet (the zero energy is taken as the O_2 molecule not interacting with the system). The CG minimization curve decreases down to -3.69 eV, where molecular adsorption takes place. In the present case, both O atoms in the molecule are interacting with the two neighboring C atoms. As in the previous case, the dissociation of the molecule in a configuration close to the molecular adsorption state was considered. In this case, the CG minimization to the $O-O$ dissociated state yielded a further energy decrease of -3.95 eV with respect to the adsorbed molecular state. That is, the final dissociated state has an energy of -7.64 eV with respect to a reference state, where the O_2 molecule is located far away from the surface. In this final state, the TiO_2 entity remains adsorbed onto the graphene on a *rotated bridge* adsorption site with a binding energy of -1.44 eV. The Ti-O average distance is $d_{Ti-O}=1.68\pm 0.01$ Å, the O-O distance is $d_{O-O}=2.68$ Å, and the angle formed with the titanium is $\angle_{O}^{Ti-O}=105.5^\circ$.

A NEB pathway was constructed linking the present adsorbed molecular and atomic states for O, with the results shown in Fig. 2(d). The optimized reaction path presented an energy barrier of 0.11 eV, which is quite a low value. Thus, also in this case, the Ti oxidation reaction is practically a nonactivated process and it should occur rapidly at room temperature.

It is interesting to compare the previous results with the energy change of the Ti oxidation reaction:



for which we obtain a value of -7.71 eV. From this figure, and the binding energies of Ti and TiO_2 to the surface (which are very close), we see that most of the binding energy of the O_2 molecule to the surface in the dissociated state is provided by Ti oxidation.

The binding energy of the dissociated O_2 molecule was also calculated in other adsorption situations, as depicted in Figures 2(e)–2(i), with the results given in Table II. Note that the denomination given to the different adsorption situations

does not refer to the O_2 molecule, but rather to the TiO_2 molecule.

A straightforward average of binding energy values of O_2 to the Ti/graphene surface yields -7.74 ± 0.03 eV, denoting a strongly irreversible process. The values of binding energy of TiO_2 to the graphene surface are also included in the table. The average binding energy is equal to -1.54 ± 0.03 eV.

Oxidation of titanium in the presence of adsorbed hydrogen

Since O_2 can oxidize the Ti decoration, the oxidation process in the presence of a H_2 molecule stored on the system was also considered. As a starting point, a H_2 molecule adsorbed on the Ti adatom and an O_2 molecule in the gas phase were analyzed. Two possible scenarios were analyzed for the adsorbed hydrogen molecule: the dissociated state and the molecular one. Even though H_2 dissociation at low coverage of the Ti/graphene system presents an energy barrier, calculations with different system sizes show that this barrier decreases as Ti coverage increases, so that dissociation tends to be more probable for larger Ti coverage.

The first set of CG calculations was performed starting with the dissociated hydrogen molecule adsorbed onto the Ti and the O_2 molecule not interacting with the system. The oxygen molecule was allowed to approach the Ti adatom from an adjacent side in a direction parallel to the surface. Figure 3(a) shows the energy changes during the CG minimization steps. The final state of this procedure corresponds to the molecular adsorption of O_2 with an energy gain of -3.34 eV, while the hydrogen atoms remain in the dissociated state. Since we know from the results presented above that O_2 may occur in an atomic dissociated state, separated from the molecular state by an activation barrier, we prepared a final state by means of CG minimization where the TiO_2 is formed and the H_2 is present in molecular state. This configuration can be observed in the inset of Fig. 3(b). We then run the NEB procedure between the final state shown in Fig. 3(a) (inset, bottom right in this figure) and the state shown in the inset of Fig. 3(b). The energy along the NEB pathway is shown in Fig. 3(b). An energy difference of -3.98 eV is obtained between the initial and final states of this figure, with an energy barrier of 0.74 eV. This barrier corresponds to the titanium oxidation process in the presence of the hydrogen atoms adsorbed on the titanium. Thus, the overall energy change between the dissociated H_2 to molecular H_2 plus the dissociative adsorption of the O_2 molecule amounts to -3.34 eV + $(-3.98$ eV) = -7.32 eV. At this state, the H_2 molecule remains adsorbed on the Ti atom with a binding energy of -0.42 eV.

The other scenario corresponds to the H_2 molecule stored in a molecular way. Figure 3(c) shows the CG minimization curves. Here, the O_2 molecule also approaches the surface in a direction parallel to the graphene sheet. At the end of the CG minimization, oxygen remains adsorbed as a molecule. In this case, the energy gain is -3.95 eV. The subsequent NEB reaction pathway to give dissociated O_2 (yielding the TiO_2 entity) and adsorbed H_2 is given in Fig. 3(d). The energy change for this step is -3.76 eV, so that, in this case, the energy change for the whole process is -7.71 eV.

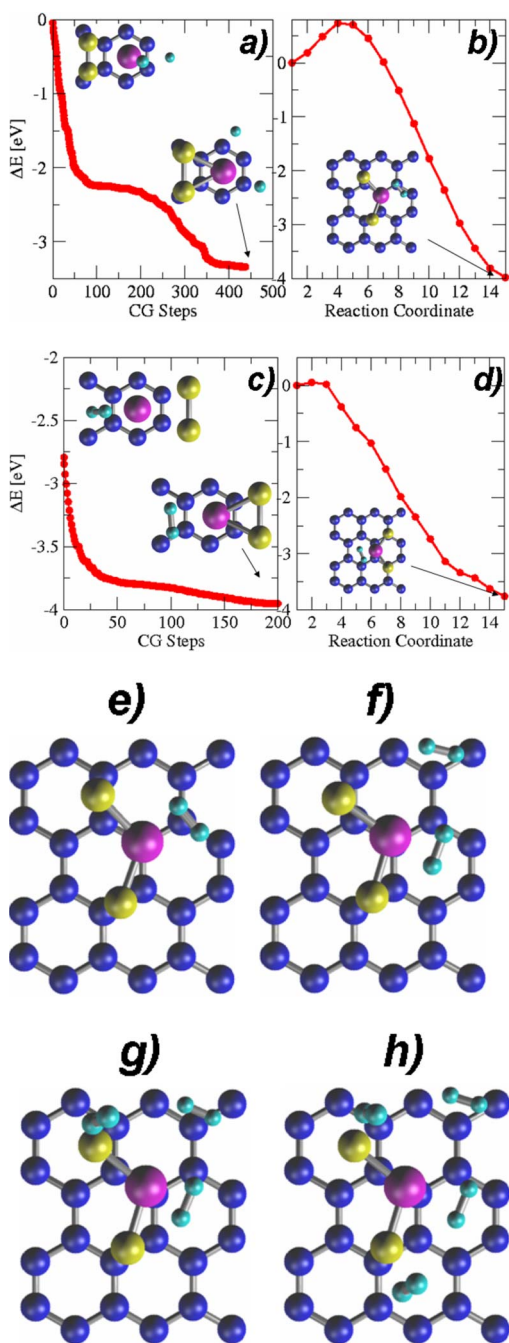


FIG. 3. (Color online) Oxidation reaction in the presence of stored hydrogen. (a) CG energy changes (eV) vs minimization steps for the molecular oxygen adsorption onto Ti in the presence of a dissociated hydrogen molecule. (b) Energy along reaction coordinate obtained with the NEB method for the O_2 dissociation reaction. The two hydrogen atoms rebuild the H_2 molecule, and titanium yields TiO_2 . The H_2 molecule remains adsorbed close to the TiO_2 . (c) CG energy changes (eV) vs minimization steps for the molecular oxygen adsorption onto Ti in the presence of an adsorbed hydrogen molecule. (d) Energy along reaction coordinate obtained with the NEB method for the O_2 dissociation reaction. The hydrogen molecule remains adsorbed during all the process. [(e)–(h)] Equilibrium configurations as obtained from CG minimization for different numbers of hydrogen molecules adsorbed on the TiO_2 /graphene system: (e) one, (f) two, (g) three, and (h) four H_2 molecules. Blue, C; magenta, Ti; yellow, O; and cyan, H.

Hydrogen storage capacity of the titanium dioxide decorated graphene surface

We have seen in the previous section that once the titanium dioxide molecule is formed, the system can still store one hydrogen molecule. Calculation with different numbers of hydrogen molecules shows that the system can coordinate up to four molecules per TiO_2 species. The resulting adsorption energies per molecule are -0.42 , -0.27 , -0.18 , and -0.11 eV/ H_2 in the case of one, two, three, and four molecules, respectively. Therefore, we find that, even in the presence of adsorbed O_2 , the Ti/graphene system may store up to four hydrogen molecules. However, only the adsorptions of the first present a binding energy comparable to the oxygen-free surface. Figures 3(e)–3(h) show the CG equilibrium configurations for the adsorption of one, two, three, and four hydrogen molecules. The TiO_2 species is adsorbed on a *rotated top* configuration. The first two hydrogen molecules arrange close to the titanium atom, and the other two adsorb close to the oxygen atoms.

Water adsorption

Since water is a major contaminant present in the air, the interaction of one and two water molecules with the Ti/graphene system was also considered. Figures 4(a) and 4(b) show the CG equilibrium configurations in the case of the adsorption of one and two water molecules. The binding energies per water molecule are -1.52 and -1.44 eV/ H_2O , respectively.

Monitoring of the two water molecules adsorbed on the Ti adatom shows that they try to reproduce the titanium dioxide configuration without losing their molecular structure. The difference in energy between the configuration of two water molecules adsorbed onto Ti/graphene (initial state) and a TiO_2 molecule plus two hydrogen molecules adsorbed on graphene (final state) is equal to -1.68 eV. Both states correspond to CG equilibrium configurations. Figure 4(c) shows the reaction path between these two states, obtained with the NEB method. In Fig. 4(c), it can be seen that the dehydrogenation reaction must overcome a large energy barrier (4.29 eV), so that at room temperature its occurrence is quite improbable. Figure 4(c) is also useful in considering the back reaction; hydrogen uptake by a TiO_2 molecule adsorbed on graphene. From this figure, this reaction should both be thermodynamically and kinetically disfavored. However, the present results only consider one possible reaction path, and more detailed study is required to provide a clear-cut answer.

Nitrogen adsorption

The major air component, nitrogen, was also considered. Figure 4(d) shows the adsorption steps for a nitrogen molecule during a CG minimization.

The noninteracting N_2 molecule has N-N distance of $d_{N-N} = 1.15$ Å. At the beginning of the minimization, the N_2 molecule approached the Ti adatom from an adjacent side in a direction parallel to the sheet. The energy decreased quickly and monotonically to the end point, with a final value of -1.17 eV. At this point, the N-N distance and the

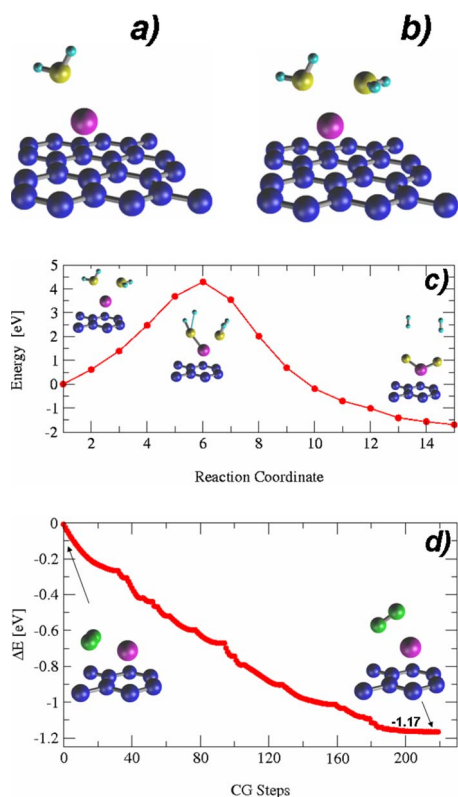


FIG. 4. (Color online) CG equilibrium configurations for the adsorption of (a) one and (b) two water molecules adsorbed on the Ti/graphene system. (c) Energy along the reaction coordinate as obtained with the NEB method for the oxidation of Ti by two water molecules. The energy zero is taken at the initial state. (d) CG equilibrium configuration for the adsorption of nitrogen on Ti/graphene: Blue, C; magenta, Ti; yellow, O; cyan, H; and green, N.

average Ti-N distance were $d_{N-N}=1.25 \text{ \AA}$ and $d_{Ti-N}=2.05 \pm 0.02 \text{ \AA}$, respectively. The adsorption of the N_2 molecule onto the Ti/graphene system is a molecular one, as shown in Fig. 4(d).

CONCLUSIONS

Motivated by the possible application of Ti-modified carbon nanotubes to store hydrogen at high densities, we performed DFT calculations of Ti-modified graphene layers in contact with different adsorbates that may compete with hydrogen in the adsorption process. The use of a graphene layer

circumvented the large computational requirements of nanotubes and delivered qualitatively similar results to those previously reported in the literature for hydrogen adsorption. Therefore we estimate that present conclusions may be qualitatively extrapolated to the case of nanotubes. The main conclusions are as follows:

(1) The decoration of the graphene sheet with Ti allows storing up to four hydrogen molecules per adatom with an average binding energy of $-0.42 \text{ eV/molecule}$. These results, which represent a considerable improvement with respect to the carbon system, are practically identical to those obtained in calculations for carbon nanotubes in the literature.

(2) An oxygen molecule behaves as a very reactive species toward Ti adsorbed on graphene. It should oxidize spontaneously the titanium adatom to titanium dioxide, and it remains chemisorbed onto the graphene with a chemical binding energy close to -8 eV , a huge energy amount.

(3) Small amounts of oxygen present in the 2H/Ti/graphene system are expected to yield the oxidation of the titanium adatom to titanium dioxide, changing the adsorption site to a top rotated position. The resulting titanium dioxide would bind to the graphene sheet with a strong chemical bond. In the presence of TiO_2 , the energy barrier to form the H_2 molecule from adsorbed atomic hydrogen is reduced to 0.74 eV from a value of 1.74 eV when only Ti decorates the graphene layer.

(4) The titanium dioxide could coordinate up to four hydrogen molecules, which remain physisorbed to it with a weak bonding. However, only the first two hydrogen molecules present an interesting binding energy to the surface.

(5) One and two water molecules adsorb on Ti/graphene without dissociation. They attempt to reproduce the titanium dioxide configuration without losing their water structure. The binding energy of these molecules is of the order of -1.5 eV .

(6) The nitrogen molecule adsorbs on the titanium without dissociation, also with a binding energy of -1.17 eV .

ACKNOWLEDGMENTS

This work was supported by PIP 5901/05 CONICET, Program BID 1728/OC-AR PICT 06-12485 and PICTOR 936, Agencia Córdoba Ciencia, and SECyT UNC, Argentina. We wish to thank J. F. Junquera for the explanation and bibliography on the basis sets. Language assistance by C. Mosconi is also acknowledged.

*Corresponding author. FAX: +54-351-4344972. eleiva@fcq.unc.edu.ar

¹S. Li, Z. Yu, R. Rutherglan, and P. J. Burke, *Nano Lett.* **4**, 2003 (2004).

²R. Saito, M. Fujita, G. Dresselhaus, and M. S. Dresselhaus, *Appl. Phys. Lett.* **60**, 2204 (1992).

³H. Dai, *Surf. Sci.* **500**, 218 (2002).

⁴M. Ouyang, J. L. Huang, and C. M. Lieber, *Acc. Chem. Res.* **35**, 1018 (2002).

⁵C. L. Kane and E. J. Mele, *Phys. Rev. Lett.* **78**, 1932 (1997).

⁶Y. Zhang, N. W. Franklin, R. J. Chen, and H. Dai, *Chem. Phys. Lett.* **331**, 35 (2000).

⁷E. Durgun, S. Dag, V. M. K. Bagci, O. Gülseren, T. Yildirim, and S. Ciraci, *Phys. Rev. B* **67**, 201401(R) (2003).

- ⁸T. Yildirim and S. Ciraci, Phys. Rev. Lett. **94**, 175501 (2005).
- ⁹P. Ordejón, E. Artacho, and J. M. Soler, Phys. Rev. B **53**, R10441 (1996).
- ¹⁰J. M. Soler, E. Artacho, J. D. Gale, A. García, J. Junquera, P. Ordejón, and D. Sánchez-Portal, J. Phys.: Condens. Matter **14**, 2745 (2002).
- ¹¹J. P. Perdew, K. Burke, and M. Ernzerhof, Phys. Rev. Lett. **77**, 3865 (1996).
- ¹²N. Troullier and J. L. Martins, Phys. Rev. B **43**, 1993 (1991).
- ¹³L. Kleinman and D. M. Bylander, Phys. Rev. Lett. **48**, 1425 (1982).
- ¹⁴S. G. Louie, S. Froyen, and M. L. Cohen, Phys. Rev. B **26**, 1738 (1982).
- ¹⁵J. Junquera, O. Paz, D. Sánchez-Portal, and Emilio Artacho, Phys. Rev. B **64**, 235111 (2001).
- ¹⁶W. H. Press, B. P. Flannery, S. A. Teukolsky, and W. T. Vetterling, *Numerical Recipes: The Art of Scientific Computing* (Cambridge University Press, Cambridge, 1986).
- ¹⁷G. Henkelman, B. P. Uberuaga, and H. Jonsson, J. Chem. Phys. **113**, 9901 (2000).
- ¹⁸G. Henkelman and H. Jonsson, J. Chem. Phys. **113**, 9978 (2000).
- ¹⁹Y. Baskin and L. Mayer, Phys. Rev. **100**, 544 (1955).
- ²⁰*Handbook of Chemistry and Physics*, 80th ed. edited by David R. Lide (CRC, Boca Raton, FL, 2000).
- ²¹M. V. Ramana and D. H. Phillips, J. Chem. Phys. **88**, 2637 (1988).